Seasonal-scale Transport Patterns in a Multi-inlet Coastal Lagoon

N. P. Smith

Harbor Branch Oceanographic Institution, 5600 U.S. Highway 1 North, Fort Pierce, FL 34946, U.S.A.

A finite-difference numerical model is used to investigate seasonal-scale lagoon-shelf exchanges and transport within Indian River, a multi-inlet lagoon on the Atlantic coast of Florida, U.S.A. Meteorological, hydrologic and hydrographic data quantify forcing by seasonally-varying wind stress, coastal sea level and the net freshwater gain. The along-axis component of the wind stress reverses seasonally. North-westward wind stress stores water in the northern part of the lagoon in summer months, then south-westward wind stress removes it in winter months. The seasonal rise and fall in water level at opposite ends of the lagoon differ by $\pm 0{\cdot}1$–$0{\cdot}2$ m, primarily as a result of seasonal variations in wind forcing. The rise and fall of coastal sea level forces water into the lagoon during summer months, then draws it out during late fall and winter months. Net freshwater gain forces water out of the inlets during summer months, when rainfall rates are highest, and to a lesser extent during mid winter, when evaporation is relatively low. When forcing is by shelf tides only, simulations suggest that the northern and southern inlets are flood-dominant, while the central inlet is ebb-dominant. With the addition of seasonal-scale forcing, the northern inlet becomes flood-dominant from late fall through early spring, then ebb-dominant during the rest of the year. The central and southern inlets are ebb-dominant throughout the year but seasonal variations differ. The central inlet has strongest outflow during summer months, while the southern inlet has strongest outflow during fall and winter months. Convergent and divergent patterns of transport within the lagoon are a complex response to both local and remote forcing. Simulations suggest that transport in the dredged part of a navigation channel opposes transport outside the channel.

Keywords: coastal lagoons; seasonal variations; models; transport; tidal inlets; Florida coast

Introduction

Shallow lagoons are a common feature of coastal environments. Barnes (1980) has estimated that 13% of all coasts are lined with lagoons. Lagoons are typically found along microtidal coasts with flat coastal plains and broad continental shelves (Bird, 1994). They are relatively young features, having formed over the last 5000–7000 years, and they are often short-lived over geological time scales due to sedimentation (Martin & Dominguez, 1994). Tropical lagoons in particular play an important ecological role, because of their high primary and secondary productivity (Krumbein *et al.*, 1981). Understanding the circulation within a lagoon and natural flushing by lagoon-shelf exchanges is fundamental to maintaining its ecological health as well as its economic value.

Coastal lagoons are highly responsive to wind forcing, because of their characteristically large surface area to depth ratio, and currents are quickly damped by bottom friction. Tide-induced residual transport (Smith, 1990*a*) is a quasi-steady and predictable component of the circulation in the interior of a lagoon, but even normal wind forcing can dominate and reverse tidal transport (Smith, 1990*b*). The low-frequency movement of water through the inlets that connect a lagoon with shelf waters is generally less apparent than tidal transport, but it is an important component of the circulation. Transport over time scales ranging from days to seasons contributes to the dispersion of dissolved and suspended material, thereby playing a significant role in flushing the lagoon and maintaining water quality.

If a lagoon has a single inlet connecting it with inner shelf waters, the basin responds in a pumping, or Helmholz mode at tidal and subtidal frequencies (Spaulding, 1994). Subtidal-frequency exchanges are almost exclusively in response to the slow rise and fall in sea level, which can be a response to winds, currents and atmospheric pressure gradients (Wong, 1991). Low-frequency exchanges through inlets can also occur from fortnightly and monthly interactions of diurnal and semidiurnal tidal constituents, as the lagoon alternately fills and drains in response to variations in tidal pumping (Hill, 1994). Low-frequency outflow through inlets varies seasonally as a time-lagged response to local rainfall and regional runoff.

E-mail: nsmith@hboi.edu

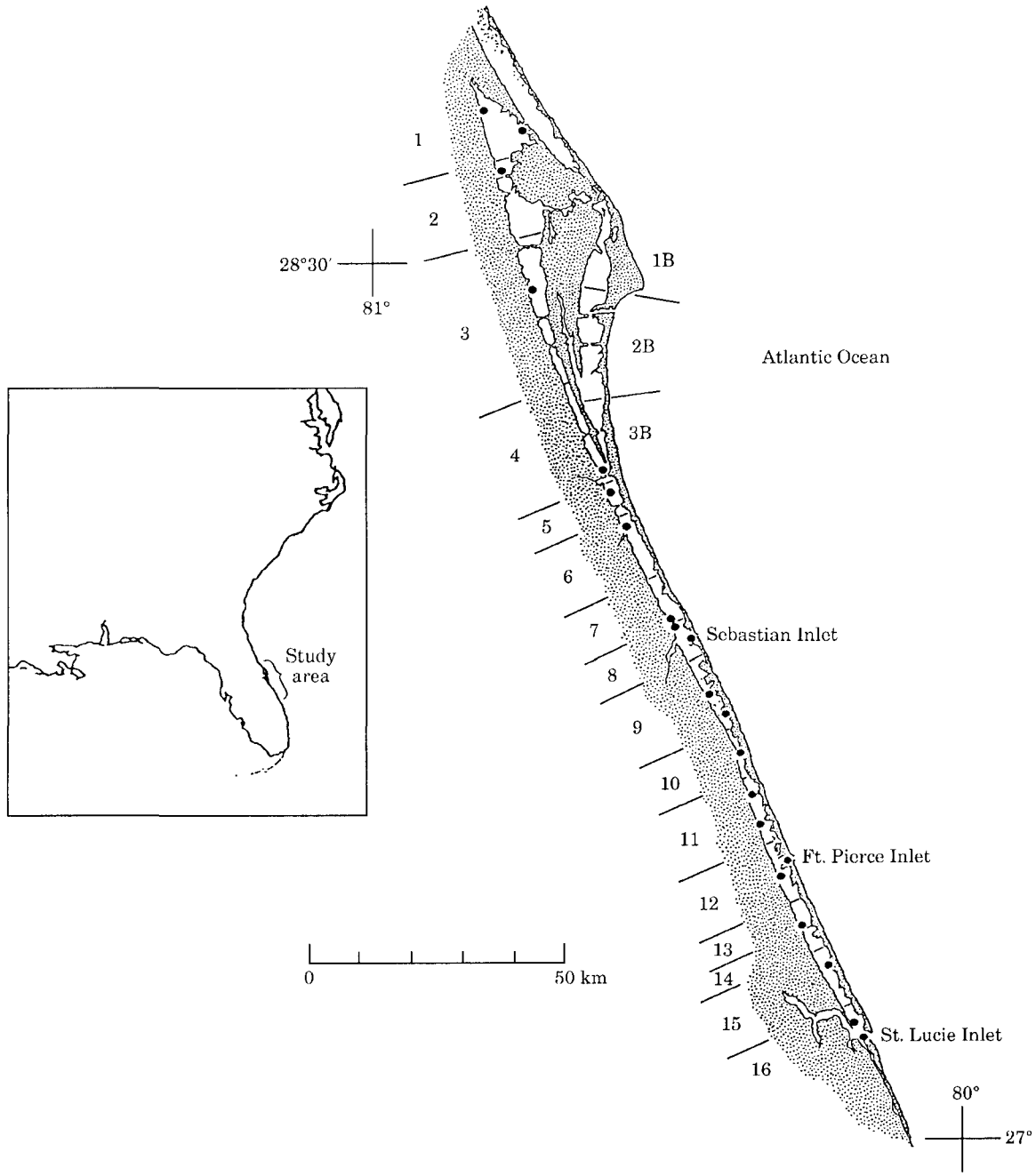

FIGURE 1. Indian River lagoon and Banana River lagoon, along the Atlantic coast of the Florida Peninsula. Numbers landward of Indian River (1–16) and seaward of Banana River (1B–3B) indicate the segments defined for the finite difference model. Solid circles represent study sites at which water level records were available for model validation.

A lagoon with multiple inlets can respond to low-frequency fluctuations in coastal sea level with simultaneous inflow and outflow (Wong & Wilson, 1984), but transport patterns can become an intricate response to tidal and nontidal processes. Wiseman and Inoue (1993) reported that the response to fluctuations in coastal sea level can be influenced significantly by local wind forcing when the set-up and set-down of water levels at opposite ends of a multi-inlet estuary influence the estuarine-shelf water level difference. Differences in inlet geometry or tidal forcing can effect a baseline level of transport through

the inlets, and thus through the interior. For similar tidal conditions at the inlets, the residual flow within the lagoon due to inlet size is in the direction of the inlet that offers the greatest resistance to tidal exchanges. Inlet resistance can be a result of a longer channel, shallower depth or narrower width. Van de Kreeke and Cotter (1974) demonstrated this with an analytical model representing a lagoon with an inlet at each end. Conversely, for similar sized inlets, a net inflow will occur through the inlet that has the larger tidal amplitude (Liu & Aubrey, 1993), and the residual flow within the lagoon will be toward the inlet with the smaller amplitude. Throughout the lagoon, tide-induced transport will increase and decrease as tidal constituents cycle in and out of phase.

Indian River is a microtidal lagoon that lies along the Atlantic coast of Florida (Smith 1987, 1990*c*, 1992). The lagoon is 195 km long, the average width is about 3 km and the average depth is 1·7 m. The longitudinal axis of the lagoon is oriented approximately 340–160° (Figure 1). Three inlets in the southern half of the lagoon can be used to define three sub-basins. The northern sub-basin is north of Sebastian Inlet, which is 82 km north of the southern end of the lagoon and 15 km south of the midpoint. Approximately 71% of the surface area of Indian River is north of Sebastian Inlet. Banana River lagoon, connected at its southern end to the midpoint of the northern sub-basin, has a length, width and average depth of 54 km, 3 km and 1·4 m, respectively. The central sub-basin lies between Sebastian Inlet and Fort Pierce Inlet. Fort Pierce Inlet is 45 km south of Sebastian Inlet and 37 km north of St. Lucie Inlet. The southern sub-basin is bounded by Fort Pierce Inlet and St. Lucie Inlet.

On an average tidal cycle, approximately 39×10^6 m^3 of water enters and leaves Indian River (Smith, 1992). Fort Pierce Inlet is the largest inlet, transporting just over 50% of the intertidal volume. Sebastian Inlet and St. Lucie Inlet exchange approximately 30% and 20% of the intertidal volume, respectively. Circulation studies of Indian River over the past 20 years have documented both the direct response to wind forcing (Smith, 1990*c*) and an upwind return flow in the dredged part of the Atlantic Intracoastal Waterway (Pitts, 1989, 1996; Smith, 1990*c*). The return flow is most apparent in the northern sub-basin where the barotropic pressure gradient associated with the set-up or set-down of water level at the northern end of the lagoon is well defined.

The purpose of this paper is to show that seasonal-scale meteorological, hydrologic and hydrographic forcing can distort baseline tide-induced residual flow patterns significantly. Results suggest that nontidal transport varies substantially over seasonal time scales, and that inlets can alternate between flood-dominant and ebb-dominant. Also, water that is stored seasonally in the northern end of the lagoon perturbs the seasonal rise and fall in water level relative to that in the southern part of the lagoon and in shelf waters.

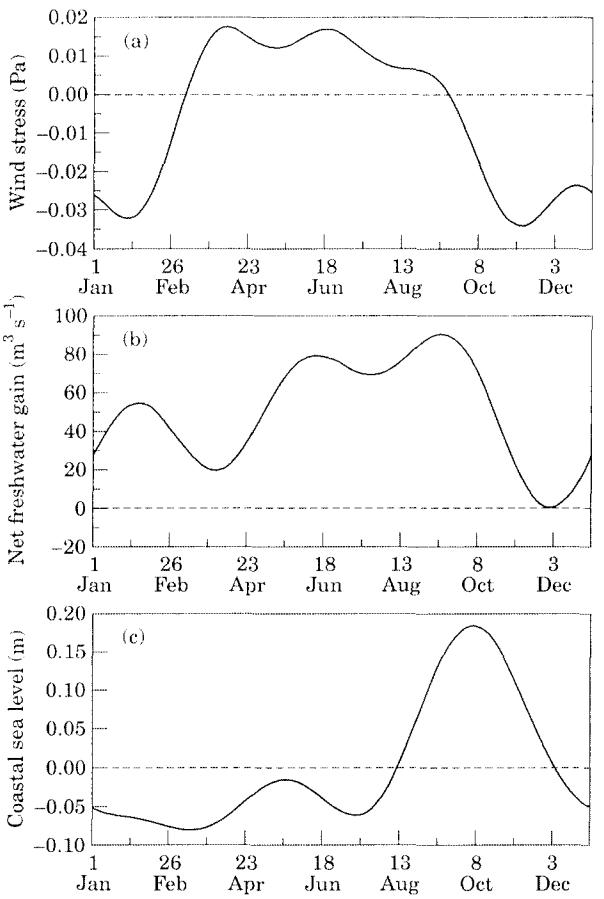

FIGURE 2. Along-axis component (340–160°) wind stress (a), net freshwater gain (b) and coastal sea level (c) for an average year, as defined by multi-annual meteorological, hydrologic and hydrographic data.

Data

Climatological data, including monthly mean wind speeds and prevailing directions, are available from coastal weather stations along the northern (NOAA, 1970*a*,*b*) and central (NOAA, 2000) parts of the lagoon. Multi-annual monthly sea levels from Daytona Beach and Miami Beach (Permanent Service on Mean Sea Level, 1977) provide an estimate of the rise and fall of coastal water levels over seasonal time scales in the study area. Harmonic constants for the

principal semidiurnal and diurnal tidal constituents (M_2, S_2, N_2, K_1, O_1 and P_1) are available from the studies in shelf waters off all three inlets (Smith, 1992). M_2 is the primary constituent with an amplitude of 0·46 m. The other five constituents have amplitudes of between 0·04 and 0·11 m. Seasonal cycles of the net freshwater gain, incorporating precipitation, runoff, groundwater seepage and evaporation, are estimated from hydrologic data reported by Glatzel (1986), Rao (1987) and (Glatzel & DaCosta, 1988). Unpublished multiannual mean runoff values were available for 11 creeks and drainage canals emptying into eight of the 16 segments of Indian River.

Methods

Monthly values of mean wind speed and prevailing direction were decomposed into components parallel (340–160°) and perpendicular to the axis of Indian River lagoon. The along-axis component was used to quantify wind forcing. Harmonic analysis (Panofsky & Brier, 1963) of monthly along-axis wind components provided amplitudes and phase angles needed to construct a smoothly varying annual cycle of hourly values. Surface wind stress was quantified using the drag coefficient suggested by Wu (1980). Monthly mean values of coastal sea level, rainfall and evaporation were used in a similar way to construct annual cycles of hourly values. Harmonic analysis indicated that the seasonal rainfall curve has a twin-peaked wet season. Rainfall rates rise to 146 and 157% of the multiannual mean value on 12 June and 11 September, respectively, and drop to 63 and 23% of the mean on 30 March and 29 November, respectively. It is assumed that runoff and groundwater seepage vary seasonally, in phase and in direct proportion to rainfall. Groundwater seepage is poorly understood. A few direct measurements are available from Pandit and El-Khazen (1990), but groundwater seepage was adjusted without observational support to produce a multi-year steady state condition for salinity. The seasonal cycle of evaporation includes minimum rates of about 0·26 cm d^{-1} in December and January and maximum rates of approximately 0·5 cm d^{-1} from April through August. Freshwater gains from rainfall, runoff and groundwater seepage, corrected for evaporative losses produce the annual cycle of net freshwater gain [Figure 2(b)].

A two-layer finite difference numerical model simulated seasonal transport patterns within Indian River lagoon and through the three inlets in response to tidal, hydrologic and meteorological forcing. Indian River lagoon was sub-divided into 16 segments (Figure 1), according to the availability of water level data needed to verify simulations. Segment surface areas varied from 12·7 to 87·5 km^2 and averaged 35·5 km^2. The upper layer extends from the western shore to the eastern shore. A 50-m wide lower layer represents the dredged part of the Atlantic Intracoastal Waterway (AIW), a navigational channel with a depth of 3·5 m that runs along the entire length of the lagoon. Banana River lagoon, attached to Segment 4 of Indian River lagoon, was divided into three segments with an average surface area of 58·7 km^2. Banana River has no dredged navigational channel.

The momentum equation used to calculate longitudinal flow in the upper layer is

$$\frac{\Delta u}{\Delta x}=\frac{\tau_x}{\rho Z}+g\frac{\Delta Z}{\Delta x}+\frac{gZ_m}{\rho}\frac{\Delta \rho}{\Delta x}-C_D\frac{u|u|}{Z}, \qquad (1)$$

where u is the flow in the x-direction, along the axis of the lagoon, τ is wind stress, g is gravity, ρ is density, C_D is the drag coefficient, and Z and Z_m are the total water depth and mid water column depth of the segment. Shelf tides, combined with the seasonal rise and fall in coastal water level, are specified at the mouth of each inlet. The surface slope defining the barotropic pressure gradient within the lagoon and in the inlets is modified by local freshwater gains and losses due to local rainfall and evaporation, freshwater runoff through drainage canals and groundwater seepage. Quadratic bottom friction is applied to the entire width of the upper layer, but an eddy viscosity term, K_z (Bowden & Hamilton, 1975), replaces the wind stress term in (1) in the momentum equation for the lower layer. Momentum equations for transport through the inlets and between Indian River and Banana River do not include wind stress terms. Transport in these connecting channels is calculated in response to friction and baroclinic and barotropic pressure gradients only.

Water density in the baroclinic pressure gradient term is a function of salinity only. The salinity of inner shelf waters is poorly documented. An annual mean value of 34 is used, with seasonal deviations of ± 1 varying inversely with rainfall. Salinity within the lagoon is controlled by the local precipitation-evaporation balance, freshwater runoff, groundwater seepage and advective transport. The model assumes instantaneous and complete mixing when water enters a segment.

The continuity equation used in the model is similar to the storage equation used in hydrologic models:

$$\frac{dV}{dt}=R+D-E+A+G, \qquad (2)$$

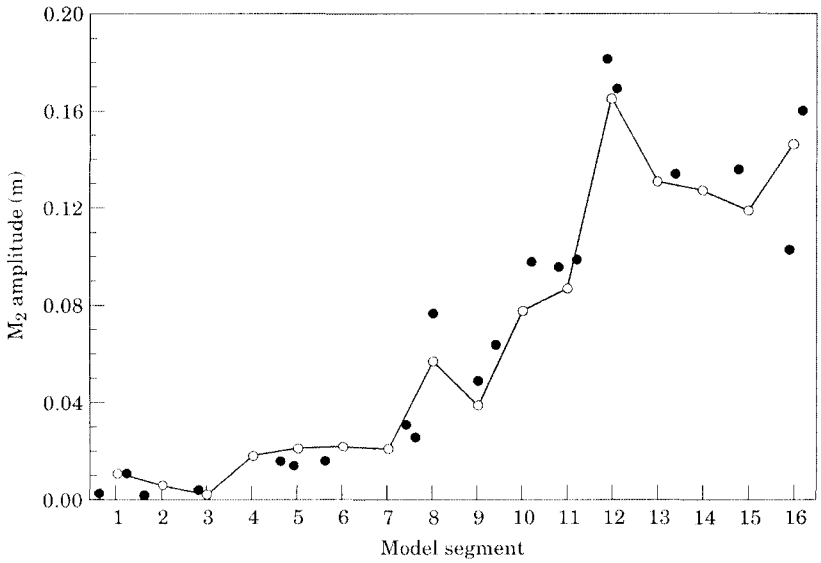

FIGURE 3. Observed (solid circles) and simulated (open circles) M_2 amplitudes for model Segments 1–16. See Figure 1 for segments and water level study sites. For plotting purposes, model segments are equally spaced.

where V is the volume of the segment, R is the rainfall rate, D is freshwater discharge into the segment, E is the evaporation rate, A is the net advective gain through the ends of the segment (including exchanges with Banana River and through the inlets), and G is groundwater seepage.

The salinity distribution used to initialize the one-year simulation was that which represents the time-varying balance between freshwater gains and losses and longitudinal mixing on 1 January. In the well-flushed southern half of the lagoon (Smith, 1993), initial salinities were generally 33–34, while at the northern end of the lagoon salinities were 36–37. During the one-year simulation, salinity remained relatively stable in the southern and central sub-basins. At the northern end of the northern sub-basin, salinity rose to an annual maximum of 38·6 in early May, then decreased to an annual minimum of 34·5 in mid-October at the end of the wet season.

Flow patterns through the interior of Indian River and through the inlets are summarized by cumulative net volume transport diagrams. By definition, transport through the inlets is positive when the flow is into the lagoon. One-year simulations were made with time steps of 180 s. Meteorological and hydrologic forcing were updated hourly. Results are presented for 1999. Because of the long time steps and thus the short run times, a one-year simulation for 1998 was used to spin-up the model and provide initial conditions for 1999.

Results

Seasonal forcing

Figure 2 summarizes the seasonal forcing for an average year that was used to drive the simulations. The along-axis component of wind stress [Figure 2(a)] is positive (north-northwestward) from March through September and negative during the rest of the year. Net freshwater gain [Figure 2(b)] peaks briefly in early February, largely because evaporation is low at that time of year. Seventy percent of the annual rainfall is recorded from May through October. Because evaporation rates are higher during summer months, however, only 66% of the annual net freshwater gain is received during the same time period. In late fall, at the start of the dry season but while evaporation is still high, the net freshwater gain becomes negative for about one month. The annual cycle of coastal sea level [Figure 2(c)] incorporates effects of regional, seasonal-scale wind forcing and the steric expansion and contraction of the water column. Lowest water levels occur in late March, with a second low in mid July. Highest water levels occur in mid October, with a secondary high water in late spring. Nontidal sea level is below the annual mean from mid December through mid August.

Model validation

Validation focused on the ability of the model to reproduce amplitudes of the M_2 constituent of each of

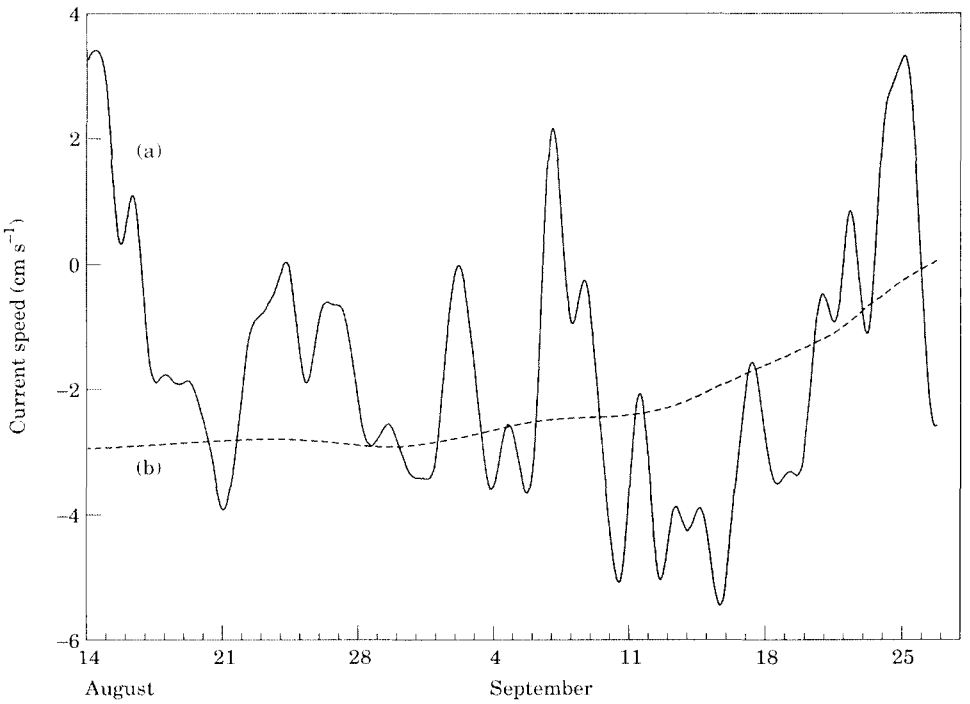

FIGURE 4. Low-pass filtered observed (a) and simulated (b) along-channel currents, representing flow in the Intracoastal Waterway 31.5 km north of Sebastian Inlet in the northern segment of Indian River. Observed currents are from 14 August through 26 September 1987; simulated currents are for the same time of year.

the 16 segments. Results are shown in Figure 3. Open circles, representing simulated M_2 amplitudes, are positioned at the midpoint of each segment. Closed circles represent M_2 amplitudes calculated from observed water level records at 21 study sites (Smith, 1987), and they are plotted north or south of the midpoint according to their location in the segment.

The model reproduces the low amplitudes observed in the northern part of the lagoon. Simulated amplitudes everywhere are within 0·05 m of amplitudes calculated from observations. In Segment 8, including Sebastian Inlet, one observed M_2 amplitude is 0·02 m larger than the value simulated for the segment. The observations came from a study site near the mouth of the inlet, however, while the simulated value represents the interior of the lagoon as well as the inlet. The poorest match appears at the southern end of the lagoon (Segment 16), where the simulated amplitude deviates from an observed amplitude by just over 0·04 m.

Validation of transport simulations through inlets and in the interior were compromised by the lack of a complete data base needed to quantify the forcing as well as the response. Figure 4 is a comparison of observed (a) and simulated (b) flow in the Intracoastal Waterway at a study site near the boundary between Segments 4 and 5, 31·5 km north of Sebastian Inlet. Observations have been low-pass filtered (Groves, 1955) to emphasize the low-frequency fluctuations that are not simulated by the model, as well as the seasonal-scale fluctuations that are. Measurements were made during a 44-day period from 14 August through 27 September, 1987. Multiannual mean meteorological and hydrologic forcing was used for the model simulation, while the observations are a response to forcing unique to the study period. Nevertheless, the two curves are fundamentally similar. Mean simulated and observed flows are negative, indicating a southward flow in the Intracoastal Waterway. The mean of the low-pass filtered observations is $-0{\cdot}017$ m s^{-1}, and the mean of the low-pass filtered simulations is $-0{\cdot}023$ m s^{-1}. Figure 4 is important for showing what the model does not include. Low-frequency transport at the time and place of this study is a continuous feature of the plot, but it is generally quite small. The root-mean-squared deviation of the observations from the simulated flow is 0·021 m s^{-1}.

Wind data from a weather station on the west side of Segment 11 were available for a 16-day time period when currents were measured near the interface between Segments 11 and 12. The predicted shelf tide was superimposed onto the seasonal mean water level,

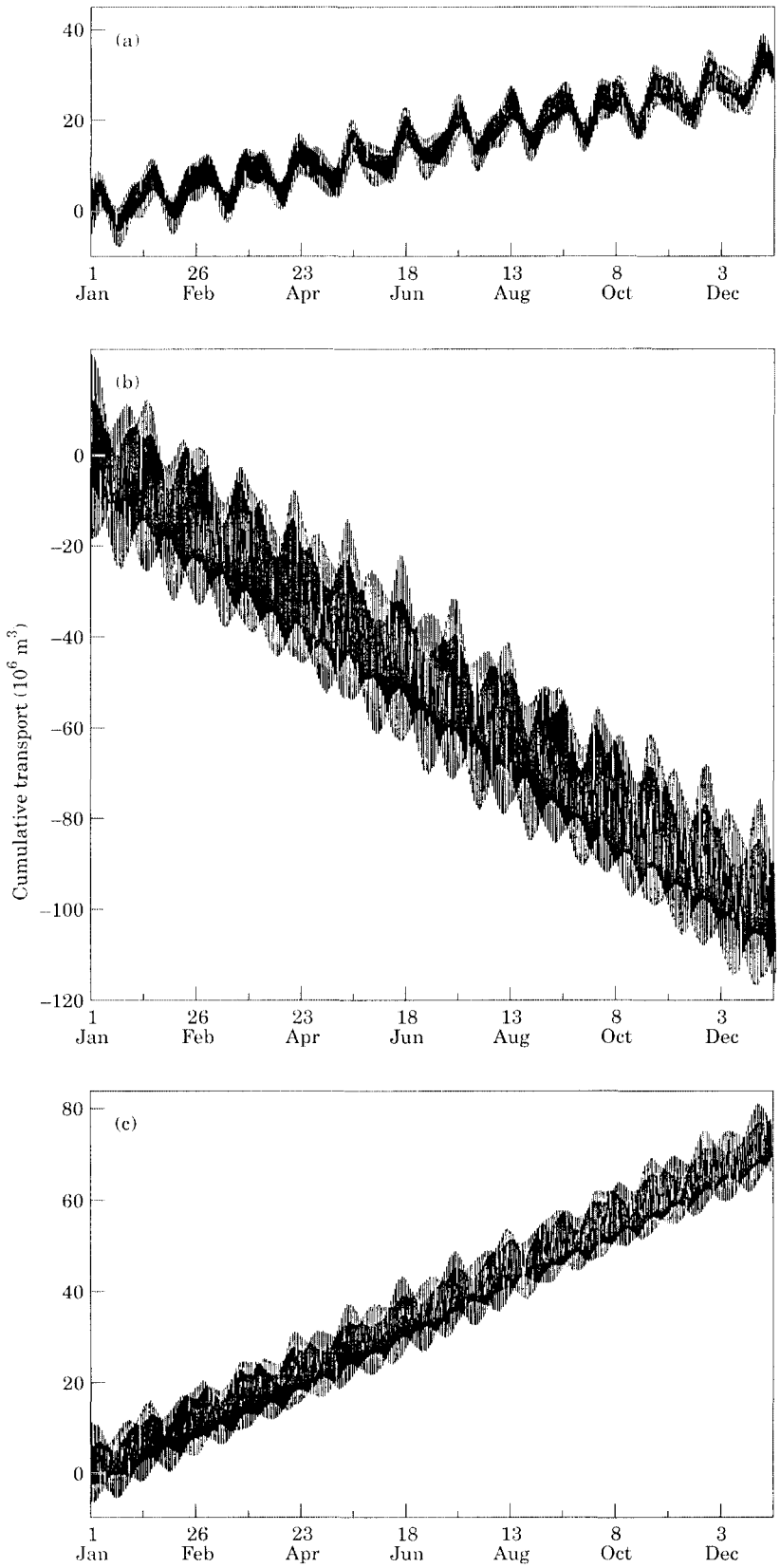

FIGURE 5. Cumulative transport through Sebastian Inlet (a), Fort Pierce Inlet (b) and St. Lucie Inlet (c) in response to tidal forcing only. Positive transport indicates flow into Indian River lagoon.

TABLE 1. Results of harmonic analyses of volume transport calculations for Sebastian Inlet, Fort Pierce Inlet and St. Lucie Inlet. Amplitudes of the principal constituents, in $m^3 s^{-1}$, are calculated from one-year simulations of lagoon-shelf exchanges

		Tidal Constituent				
		M_2	S_2	N_2	K_1	O_1
(a)	Sebastian Inlet	421	58	80	81	61
(b)	Fort Pierce Inlet	1605	223	309	300	223
(c)	St. Lucie Inlet	702	97	133	128	95

and the simulation used multiannual average rainfall, runoff, seepage and evaporation. Simulated tidal exchanges (not shown) are 60–80% of values obtained from measurements. This may be partly due to the fact that measured currents were near the top of the dredged part of the Intracoastal Waterway, while simulated currents are cross-sectional averages and thus more influenced by bottom and wall friction.

Baseline tidal transport

Although the emphasis is on seasonal variability, the model provides an opportunity to ignore the effects of seasonal-scale hydrologic and meteorological forcing and calculate the response to tidal forcing alone. This constitutes a baseline level of transport, and results provide an indication of the transport patterns that might occur when seasonal forcing becomes relatively weak. With wind forcing, net freshwater gains and seasonal fluctuations in shelf sea level all set to zero, simulations suggest that tidal forcing produces a lagoon-scale convergent pattern, with a net inflow through Sebastian Inlet and St. Lucie Inlet, and a net outflow through Fort Pierce Inlet. This in turn drives a quasi-steady transport of water within the lagoon. Results suggest also that tidal forcing maintains a set-up of water level of approximately 0·04 m within the lagoon.

The tide-induced cumulative net transport through the inlets is shown in Figure 5. The three curves are distinctly different in appearance. Model results suggest that Sebastian Inlet is flood-dominant, with a mean inflow of 0·9 $m^3 s^{-1}$. Strong monthly and, to a lesser extent, fortnightly fluctuations appear as semidiurnal and diurnal tidal constituents cycle in and out of phase. Fort Pierce Inlet has more energetic tidal exchanges (Table 1). Because of the larger tidal amplitudes, low-frequency fortnightly and monthly variations are less apparent. The mean outflow through Fort Pierce Inlet is $-3{\cdot}2$ $m^3 s^{-1}$. Large tidal transport obscures low-frequency fluctuations through St. Lucie Inlet as well. St. Lucie Inlet has a mean inflow of 2·3 $m^3 s^{-1}$.

Inlet transport patterns

Results of cumulative net transport calculations made with seasonal forcing are summarized for the three inlets in Figure 6. The patterns differ significantly from the baseline patterns when seasonal hydrologic, hydrographic and meteorological forcing is added. The pattern for Sebastian Inlet [Figure 6(a)] shows a seasonal reversal in transport, and a small net outflow at the end of the year. A seasonal net inflow occurs from late October through late March, and a net outflow occurs during the rest of the year with a maximum rate in July.

Simulations for Fort Pierce Inlet [Figure 6(b)] indicate a net export of lagoonal water that is relatively constant, except for a period of little net transport during late winter and early spring months. Strongest outflow occurs during the wet season, from late spring through late summer. For the year as a whole, the total outflow is 618×10^3 m^3, which is equivalent to about 20 $m^3 s^{-1}$.

St. Lucie Inlet [Figure 6(c)], at the southern end of the lagoon, shows a slightly more exaggerated seasonally-varying outflow. The total export of water through the inlet is 795×10^6 m^3, which is equivalent to about 25 $m^3 s^{-1}$. The seasonal cycle includes a slight inflow from mid March to late April. Strongest outflow occurs during early fall and midwinter months, when coastal sea level is decreasing rapidly (Figure 2), and when winds out of the north-easterly quadrant move water southward out of the northern part of the lagoon.

Interior transport patterns

Figure 7 shows longitudinal transport through the midpoints of the northern, central and southern sub-basins of Indian River. In each case, the curve representing transport in the dredged part of the Atlantic Intracoastal Waterway is labelled 'AIW'. The net advective transport through the middle of the northern sub-basin, between Segments 4 and 5, is northward [Figure 7(a)]. The cumulative transport at the end of the one-year simulation is $85{\cdot}1 \times 10^6$ m^3 in the upper layer and $-3{\cdot}2 \times 10^6$ m^3 in the AIW. The entrance to Banana River is just north of the southern end of Segment 4. The $81{\cdot}9 \times 10^6$ m^3 net northward advective transport occurs as a result of the $77{\cdot}5 \times 10^6$ m^3 net freshwater loss from Segments 1–4 in Indian River, the net freshwater loss from Banana

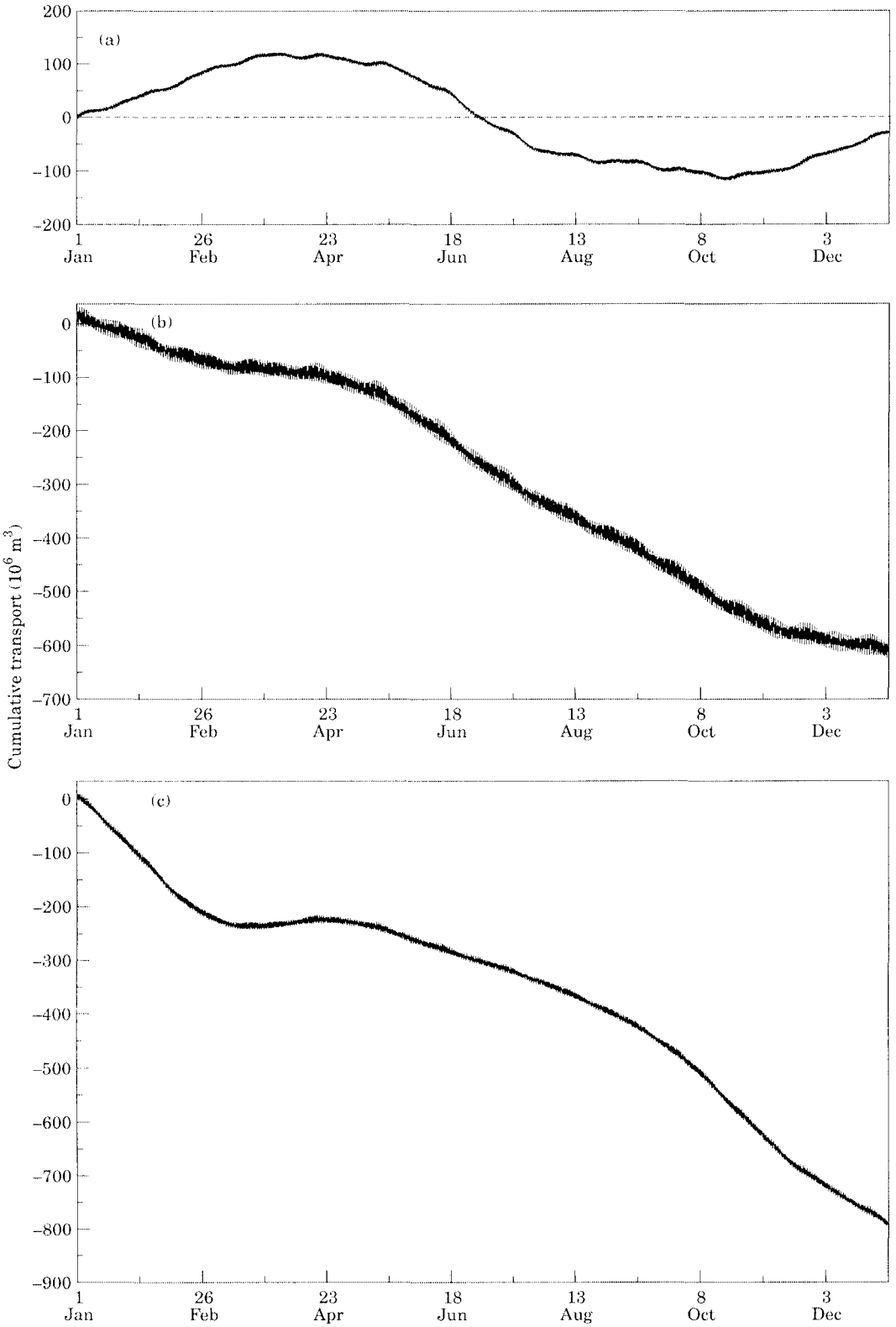

FIGURE 6. Same as Figure 5, but in response to tidal and multi-annual average seasonal-scale meteorological, hydrologic and hydrographic forcing.

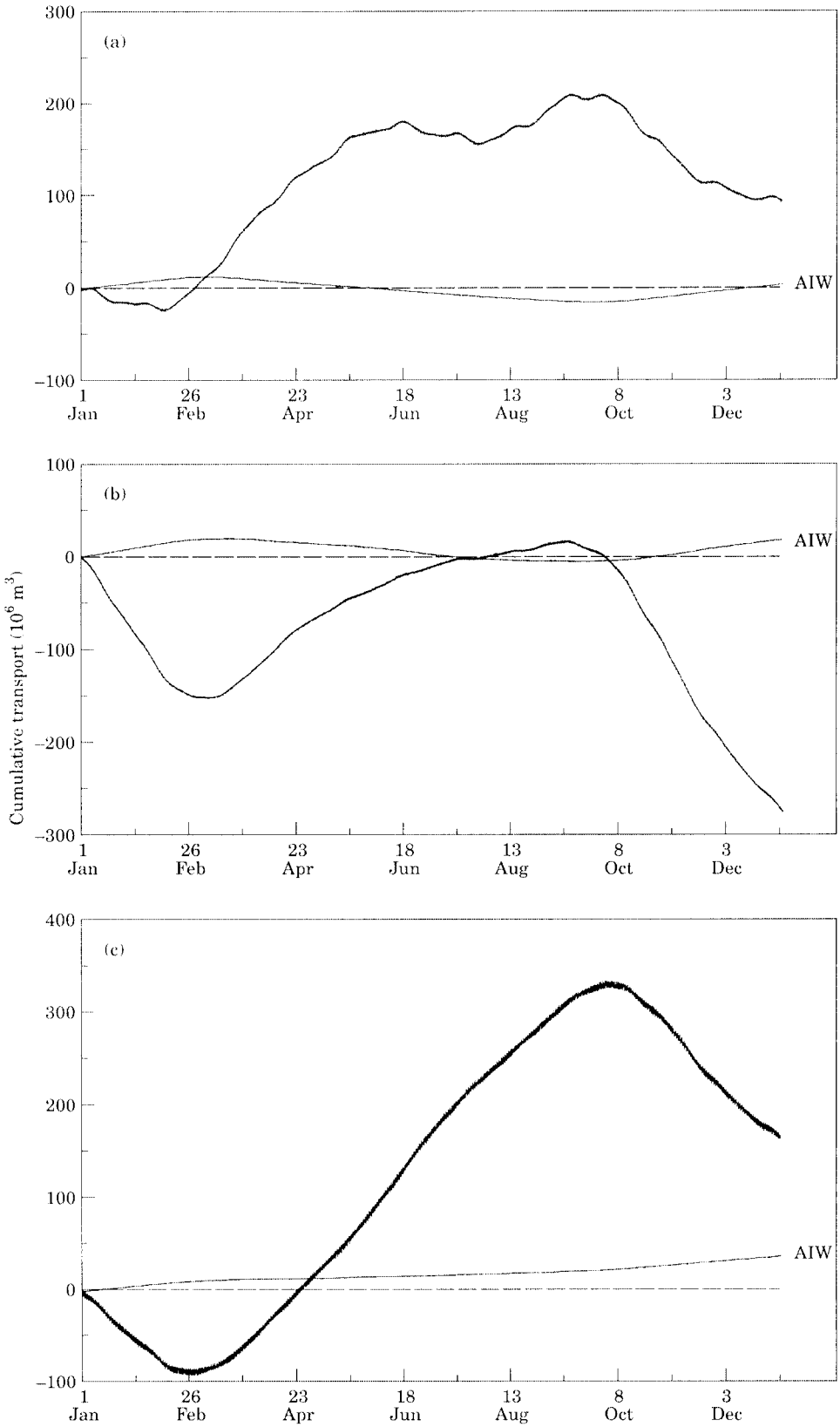

FIGURE 7. Longitudinal transport between model Segments 4–5 (a), 10–11 (b) and 13–14 (c). Positive transport indicates flow toward the north-northwest. Curves labelled AIW represents transport in the dredged part of the Atlantic Intracoastal Waterway. Note the different positions of the scale on the vertical axes.

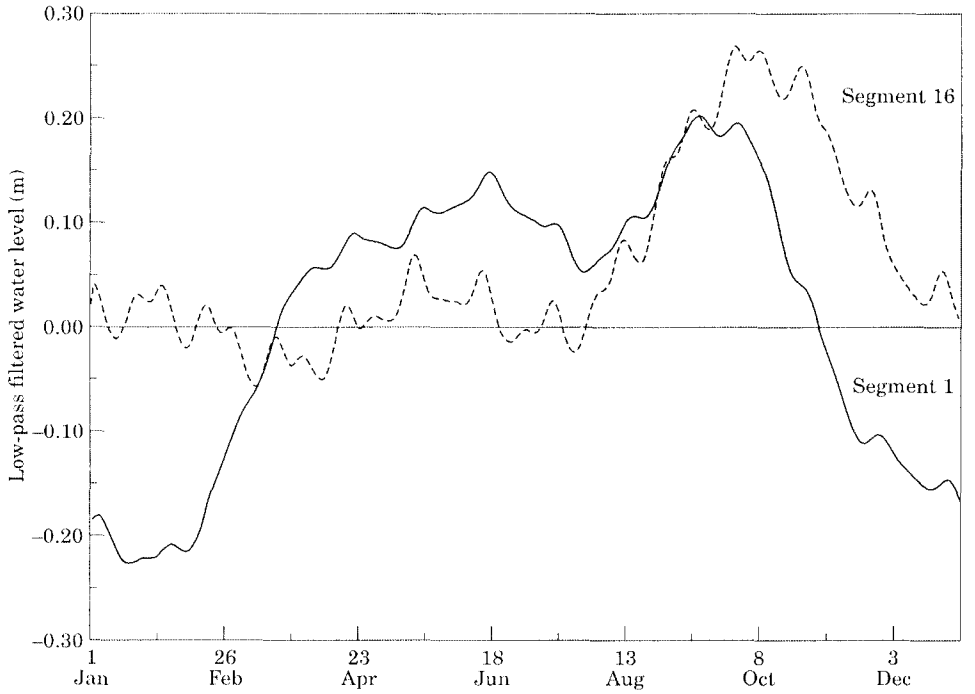

FIGURE 8. The annual cycle of water level in model Segments 1 (solid line) and 16 (broken line) in response to ocean tides and seasonal-scale meteorological, hydrologic and hydrographic forcing.

River and the slightly higher water levels at the end of the simulation. Most of the northward transport in the upper layer occurs from mid February through mid June, with a second, shorter burst from mid August through mid September. A noteworthy feature of the plot is the generally inverse relationship between transport in the upper layer and transport in the dredged part of the waterway. For example, flow in the AIW is southward from late winter through late summer, when the net flow in the upper layer is northward.

Transport between Segments 10 and 11 [Figure 7(b)] includes a net southward transport of $-282{\cdot}4 \times 10^6\ m^3$ in the upper layer and a net northward transport of $+11{\cdot}3 \times 10^6\ m^3$ in the AIW. The one-year simulation begins and ends with rapid southward transport toward Fort Pierce Inlet. Northward transport during March and April is equally rapid, but it is short-lived. Transport during summer months is northward but weak, representing a near balance between fresh water leaving the lagoon, relatively subtle fluctuations in coastal sea level and north-north-westward wind stress. Again, transport through the dredged part of the AIW is inversely related to transport in the upper layer, and the net transport in the lower layer is northward at the end of the year.

Transport through the midpoint of the southern sub-basin [Figure 7(c)] is sinusoidal in appearance, and the net transport is northward. At the end of the one-year simulation, the cumulative transport is $+162{\cdot}5 \times 10^6$ in the upper layer and $+32{\cdot}2 \times 10^6\ m^3$ in the AIW. The inverse relationship between transport in the upper layer and in the dredged part of the AIW is missing at this location, although the strongest northward flow in the AIW coincides with the southward flow in the upper layer.

Transport through the midpoint of the northern sub-basin of Indian River [Figure 7(a)] suggests that the seasonal rise and fall of water level at the northern end of the lagoon may be significantly different from that at the southern end, where the three inlets permit a relatively free exchange between the lagoon and the shelf. Figure 8 shows the hourly rise and fall of water level calculated for Segments 1 and 16. In Segment 1, although the year's lowest and highest water levels occur in mid winter and fall months, respectively, the effect of wind forcing, in combination with seasonally high freshwater gains, significantly lengthens the period of higher than average water level. At the northern end of the lagoon, the annual cycle includes a two-part maximum with a primary peak in late September and early October and a secondary peak in mid June.

In Segment 16, the annual range of water level is less, as the seasonal rise and fall more closely follows the seasonal variation of sea level in shelf waters [Figure 2(c)]. A prominent feature of the curve for Segment 16 is the rise and fall in water level over fortnightly and monthly time scales. Neither fortnightly nor monthly forcing is included in the model explicitly, but the M_2 and N_2 constituents cycle in and out of phase every 27·55 days. Similarly, the M_2 and S_2 constituents interact with a period of 14·77 days, and the K_1 and O_1 constituents interact with a period of 13·62 days. The low-frequency variations at the southern end of the lagoon occur as the tide-induced pumping of water first increases then decreases with the spring-neap or tropic-equatorial tidal cycles.

Discussion

Results suggest that seasonally varying meteorological and hydrologic forcing modulates substantially the baseline transport pattern maintained by tidal forcing in Indian River lagoon. In response to inlet size alone, Fort Pierce Inlet should be flood dominant. It is the largest inlet, and the frictional resistance to the ebb tide is not that much greater than the resistance to the flood tide. The other two inlets should be ebb dominant because they are shallower, and the frictional resistance to the ebb tide is substantially greater than the resistance to the flood. Inflow and outflow patterns arising from differences in inlet size, however, can be altered significantly by local tidal conditions, the slow rise and fall in coastal sea level, the alternation of wet and dry seasons and the wind-forced storage and removal of water from the northern segment of the lagoon. Superimposing several seasonal-scale processes onto baseline transport makes difficult the interpretation of local flow patterns, both through the inlets and within the lagoon.

The location of an inlet along the length of a lagoon also appears to be an important factor in creating net transport patterns. Tidal conditions may be similar at the seaward end of two or more inlets, but amplitudes may be quite different immediately inside the inlet, depending on whether the inlet is at the end or at some point along the length of the lagoon. Tidal waves entering through both Fort Pierce Inlet and Sebastian Inlet diverge and move north and south through the interior of the lagoon. Similarly, a convergent pattern occurs during the ebb phase of the tidal cycle. The divergence of the flood tide lowers the high tide level just inside the inlet, the convergence on the ebb tide raises the low tide level and thus the tidal amplitude is reduced. Tidal waves entering through St. Lucie Inlet can move only north, and the local decrease in tidal amplitudes is relatively small. If Indian River lagoon's three inlets were of equal size, the net tide-induced transport would be an inflow through St. Lucie Inlet and a net outflow through Fort Pierce Inlet and Sebastian Inlet. The baseline transport pattern for Indian River (Figure 5) suggests that inlet size is the dominant factor in producing the tide-induced inflow through Sebastian Inlet.

The seasonal reversal in transport through Sebastian Inlet was a surprising result of the study. The November–March period of net inflow occurs when coastal sea level is relatively low and along-axis windstress is southward. Inflow at that time of year is consistent with the baseline transport pattern, however. The midsummer period of net outflow is not consistent with the baseline transport pattern, but it occurs when the net freshwater gain is at an annual maximum. Periods of inflow and outflow through Sebastian Inlet coincide with periods of southward and northward wind forcing. Thus it does not appear that transport through Sebastian Inlet contributes to the seasonal draining or storage of water in the northern sub-basin of Indian River.

The effect of freshwater runoff probably has a disproportionate influence on St. Lucie Inlet. Hydrologic data summarized by Rao (1987) indicate that over half of the total gauged fresh water entering Indian River lagoon arrives through the St. Lucie River, directly opposite St. Lucie Inlet at the southern end of the lagoon. The large mean outflow through St. Lucie Inlet is consistent with the large local runoff. The brief period of net inflow occurs immediately following the seasonal wind shift, when water is forced northward within the lagoon (Figure 6), but before the start of the wet season, when freshwater runoff into the southern end of the lagoon increases dramatically.

For some applications, such as lagoon flushing, it would be unacceptable to exclude meteorological forcing over time scales on the order of 1–2 weeks. For the purposes of characterizing seasonal-scale lagoon-shelf exchanges and transport through the interior of the lagoon, however, this does not seem to be the case. To demonstrate this, low-frequency fluctuations in along-axis wind stress, and then low-frequency fluctuations in sea level were paired with the tidal and seasonal forcing described above. Wind stress fluctuated by $\pm 0{\cdot}05$ Pascal, and sea level fluctuated by $+0{\cdot}1$ m about the seasonal norms [see Figure 2(a and b)]. Both varied with a periodicity of 10 days. Changes in long-term net transport through the inlets were minimal. For example, when low-frequency variations in wind stress were considered, the net outflow through Fort Pierce Inlet decreased to just

over 98% of the outflow with low-frequency variations in wind stress. The net outflow through St. Lucie Inlet increased by just over 1%. When low-frequency variations in shelf sea level were included in the simulation, changes for both Fort Pierce Inlet and St. Lucie Inlet were less than 1%. The largest changes, expressed as a percent, occurred in Sebastian Inlet in response to low-frequency variations in shelf sea level. The net outflow at the end of the one-year simulation increased from -37 to -40×10^6 m^3, a change of about 8%.

It is important to keep in mind that transport through Indian River's three inlets is dominated by tidal exchanges. Transport rates associated with seasonal-scale forcing are only a small fraction of those associated with the semidiurnal and diurnal tidal constituents (Table 1). For example, the M_2 amplitude of 1605 m^3 s^{-1} through Fort Pierce Inlet corresponds to nearly 23×10^6 m^3 during the flood or ebb half of the M_2 tidal cycle. For comparison, maximum seasonal inflows and outflows through the inlet are approximately 20 m^3 s^{-1}, which is equivalent to about 450×10^3 m^3 during each half M_2 cycle. Similarly, during midyear months when Sebastian Inlet is ebb-dominant, ebb-tide volumes exceed flood-tide volumes by approximately $7{\cdot}2 \times 10^3$ m^3. This is about 0·1% of the total volume of water that leaves during the ebb half of an average semidiurnal tidal cycle. Thus, throughout the year, the opportunity is always present to export or import dissolved and suspended material with the ebb and flood of the tide. The importance of a persistent net inflow or outflow should not be underestimated, however. Accumulations can be significant when transport mechanisms operate over seasonal time scales.

Acknowledgements

Funding for this study came in part from the Florida Department of Environmental Regulation through contract number CM-118, and by the Florida Department of Natural Resources through Grant Agreement Number 6598. Support was provided also by the Atlantic Foundation. This is Harbor Branch Oceanographic Institution Contribution Nr. 1382.

References

Barnes, R. S. K. 1980 *Coastal Lagoons*. Cambridge University Press, Cambridge, 106 pp.

Bird, E. C. F. 1994 Physical setting and geomorphology of coastal lagoons. In *Coastal Lagoon Processes* (Kjerfve, B. J., ed.), Elsevier Oceanography Series, 60, Elsevier Science Publishers B.V., New York, pp.9–39.

Bowden, K. F. & Hamilton, P. 1975 Note on wind drift in a channel in the presence of tidal currents. *Proceedings of the Royal Society Series A* **219,** 426–446.

Glatzel, K. 1986 *Water budget for the Indian River lagoon: an overview of land use effects*. M.S. Thesis, Department of Oceanography, Florida Institute of Technology, Melbourne, Florida 109 pp.

Glatzel, K. & DaCosta, S. 1988 Hydrology of the Indian River lagoon. In *Indian River Lagoon Estuarine Monograph*. Marine Resources Council, Florida Institute of Technology, Melbourne, Florida.

Groves, G. W. 1955 Numerical filters for discriminating against tidal periodicities. *Transactions, American Geophysical Union* **36,** 1073–1084.

Hill, A. E. 1994 Fortnightly tides in a lagoon with variable choking. *Estuarine, Coastal and Shelf Science* **38,** 423–434.

Krumbein, W., Lasserre, P. & Nixon, S. W. 1981 Biological processes and ecology. In *Coastal lagoon research, present and future*. Report and guidelines of a seminar, Duke University Marine Laboratory, Beaufort, NC, U.S.A., August 1978. Unesco Technical Papers in Marine Science 32 pp. 53–97.

Liu, J. & Aubrey, D. 1993 Tidal residual currents through multiple tidal inlets. In *Formation and Evolution of Multiple Tidal Inlets* (Aubrey, D. & Giese, G., eds) American Geophysical Union, Washington D.C., pp. 113–157.

Martin, L. & Dominguez, J. 1994 Geological history of coastal lagoons. In *Coastal Lagoon Processes* (Kjerfve, B. J., ed.). Elsevier Oceanography Series, 60. Elsevier Science B.V., Amsterdam, pp. 41–68.

National Oceanic and Atmospheric Administration 1970*a* *Local Climatological Data, Patrick Air Force Base*. National Climatic Center, Asheville, North Carolina.

National Oceanic and Atmospheric Administration 1970*b* *Local Climatological Data, Cape Kennedy Air Force Station*. National Climatic Center, Asheville, North Carolina.

National Oceanic and Atmospheric Administration 2000 *Southeast Climatological Normals and Means, Vero Beach, Florida*. Also at URL: http://water.dnr.state.sc.us/climate/sercc/products/normals/vrb_norm.htm.

Pandit, A. & El-Khazen, C. 1990 Groundwater seepage into the Indian River lagoon near Port St. Lucie. *Florida Scientist* **53,** 169–179.

Panofsky, H. A. & Brier, G. W. 1963 *Some Applications of Statistics to Meteorology*. Pennsylvania State University, University Park, PA, 224 pp.

Permanent Service for Mean Sea Level 1977 *Monthly and annual mean heights of sea level*. Volume 2, North, Central and South America. Institute of Oceanogr. Sciences, Birkenhead, Merseyside, England.

Pitts, P. A. 1989 Upwind return flow in a coastal lagoon: Seasonal-scale barotropic transport. *Estuaries* **12,** 92–97.

Pitts, P. A. 1996 An investigation of tidal and low-frequency current processes in Florida's Indian River lagoon. *Florida Scientist* **59,** 205–215.

Rao, D. 1987 Surface water hydrology, Ch. 2. In *Indian River Lagoon Joint Reconnaissance Report* (Steward, J. & Van Armen, J., eds), St Johns River Water Management District, Plataka, Florida.

Smith, N. 1987 An introduction to the tides of Florida's Indian River lagoon I, water levels. *Florida Scientist* **50,** 49–61.

Smith, N. 1990*a* Computer simulation of tide-induced residual transport in a coastal lagoon. *Journal of Geophysical Research* **95,** 18205–18211.

Smith, N. 1990*b* Wind domination of residual tidal transport in a coastal lagoon. In *Coastal and Estuarine Studies*, vol. 38 (Cheng, R. T., ed.), Springer-Verlag, New York, pp. 123–133.

Smith, N. 1990*c* Longitudinal transport in a coastal lagoon. *Estuarine, Coastal and Shelf Science* **31,** 835–849.

Smith, N. 1992 The intertidal volume of Florida's Indian River lagoon. *Florida Scientist* **55,** 209–218.

Smith, N. 1993 Tidal and nontidal flushing of Florida's Indian River lagoon. *Estuaries* **16,** 739–746.

Spaulding, M. L. 1994 Modeling of circulation and dispersion in coastal lagoons. In *Coastal Lagoon Processes* (Kjerfve, B. J., ed.), Elsevier Oceanography Series, 60, Elsevier Science Publishers B.V., New York, pp. 103–131.

van de Kreeke, J. & Cotter, D. 1974 Tide-induced mass transport in lagoon-inlet systems. In Proceedings of the 14th International Conference on Coastal Engineering, ASCE, Copenhagen, pp. 2290–2301.

Wiseman, W. J. Jr. & Inoue, M. 1993 Local wind effects on multiple inlet estuaries. In The Science and Management of Coastal Estuarine Systems, Abstracts. International Estuarine Research Federation Conference, Hilton Head Island, South Carolina, pp. 137–138.

Wong, K.-C. 1991 The effect of coastal sea level forcing on Indian River Bay and Rehoboth Bay, Delaware. *Estuarine, Coastal and Shelf Science* **32,** 213–229.

Wong, K.-C. & Wilson, R. E. 1984 Observations of low-frequency variability in Great South Bay and relations to atmospheric forcing. *Journal of Physical Oceanography* **14,** 1893–1900.

Wu, J. 1980 Windstress coefficients over sea surface near neutral conditions—a revisit. *Journal of Physical Oceanography* **10,** 727–740.